Short Communication

Corrosion Behaviour of Powder Metallurgy Biomaterials from Phosphated Carbonyl-Iron Powders

Miriam Kupková[1,], Monika Hrubovčáková[1], Martin Kupka[2], Renáta Oriňáková[3], Andrea Morovská Turoňová[3]*

[1]Institute of Materials Research, Slovak Academy of Sciences, Watsonova 47, SK-040 01 Košice, Slovak Republic
[2]Institute of Experimental Physics, Slovak Academy of Sciences, Watsonova 47, SK-040 01 Košice, Slovak Republic
[3]Department of Physical Chemistry, Institute of Chemistry, Faculty of Science, P.J. Šafárik University, Moyzesova 11, SK-041 54 Košice, Slovak Republic
[*]E-mail: mkupkova@imr.saske.sk

Phosphate coated carbonyl-iron powders were compacted and sintered to investigate the effect of 0.5 and 1.0wt.% of phosphorus supplied through a phosphate coating on the microstructure and corrosion of sintered samples. The resultant materials consisted of spheroidized iron or iron oxide particles surrounded by a solidified liquid phase composed of various ferric phosphate compounds. The addition of phosphorus to carbonyl iron i) raised the fractal dimension of time series generated by the open –circuit potential fluctuations from 1.14 to about 1.5, ii) more than tripled the corrosion rate and iii) made the steady-state corrosion potential more noble (lower phosphorus content) or less noble (higher phosphorus content) than the corrosion potential of carbonyl-iron sample.

1. INTRODUCTION

A piece of metal can be easily converted into a complexly-shaped object with tiny and precise details. This formability and excellent mechanical properties caused that the metals are used as materials for surgical implants for more than a century. During these years, a paradigm has been established that metals intended for the use in the human body should be highly corrosion-resistant to survive the harsh physiological environment.

But as still more and more sophisticated implants appeared in order to fix the new kinds of problems, a quite general agreement has emerged that, for certain medical applications, the corrodibility can be a desirable material's property [1]. This is, for example, the case of coronary stents or synthetic scaffolds for bone tissue engineering. The mechanical support provided by a stent or scaffold is needed only temporarily for a short period after implantation, during which tissue remodelling and healing occur. After this period, implant cannot provide any beneficial effect. Contrariwise, the permanent presence of a foreign object in the body can trigger late complications such as restenosis, trombosis, etc. So, the short-term implants that provide a necessary support long enough to allow natural healing to take place and after that time decompose in situ into non-toxic corrosion products which are readily excreted from the body represent clearly preferable alternatives for the currently-used permanent implants.

Metals belonging to the biogenic elements, such as Ca, Mg, Fe, Mn, Zn are naturally present in small quantities in our body. It seems therefore reasonable to start searching for biocompatible degradable metallic materials amongst alloys based on biogenic elements.

Iron-based alloys are being actively considered as a good candidate for biodegradable medical applications. The interest is focused on alloys because the corrosion rate as well the mechanical properties of a pure iron do not meet the criteria required and therefore the corrosion rate should be modified and mechanical properties improved, e.g. by alloying.

The Fe-Mn system is investigated as a promising material for biodegradable stents [2-4], and Fe-P system seems to be interesting for the temporary replacement of bones [5,6].

Both iron and phosphorus are biogenic elements, so the implant itself and the products of its decomposition are expected to be tolerable for the human organism. And phosphorus, in addition, seems to have a beneficial effect on the interaction between Fe-P materials and osteogenic cell populations. The alloying of Fe with P enables to manipulate corrosion rate and mechanical properties. If the Fe-P material is going to be prepared by a powder metallurgy, phosphorus enables a liquid-phase sintering which increases the density of material and leads to its strengthening. The Fe-P material can be prepared with a foam-like structure resembling the bone, which enables bone tissue and blood vessels to ingrow into the implant. But to prepare the material suitable for a practical application, there is still a lot to study.

The Fe-P biomaterials considered to date were manufactured from mixtures of iron and Fe_3P powders [5,6]. This article deals with materials prepared through powder sintering process from a new class of powders – the coated powders consisting of carbonyl-iron particles coated with a layer of phosphates. The purpose of this study was to investigate how the phosphorus supplied in such a way affected both the microstructure of sintered samples and their corrosion in the Hank's solution. The sintered samples were found composed of spheroidized particles from iron or iron oxides and a solidified liquid phase surrounding these particles, consisting of various ferric phosphate compounds. It was demonstrated that the temporal evolution of corrosion potential of each freely corroding Fe-P sample yielded a time series which was a fractal with the fractal dimension of about 1.5. The correlations between this fractal dimension and the type of corrosion were discussed. The corrosion rates of Fe-P samples were estimated from the potentiodynamic polarization curves. It was found that the addition of phosphorus to iron more than tripled the corrosion rate.

2. MATERIALS AND METHODS

The carbonyl iron powder fy BASF (type CC, d50 value 3.8–5.3 μm) consisting of spherical particles composed of 99.5 % Fe, 0.05 % C, 0.01 % N and 0.18 % O was used as a starting material, the particles of which were subsequently coated with phosphates in a phosphating solution using the modified precipitation method. Phosphated iron powders were dried and calcined in air. After the procedures were completed, coated powders contained 0.5 wt.% and 1.0 wt.% of phosphorus. The samples prepared from those powders are denoted as Fe-0.5P and Fe-1.0P, respectively. Details of the applied method were presented in [7,8].

The bare and coated iron powders were cold pressed into cylindrical compacts ($\Phi10x10mm^3$) at the pressure of 600 MPa without lubricant.

The compacts were isothermally sintered in a laboratory tube furnace ANETA at the temperature of 1120ºC (Fe samples) or 1050ºC (Fe-P samples) for 60 min and cooled to the room temperature. The heating and cooling rate was kept at 10°C/min. The gas mixture of 10% H_2 – 90% N_2 (purity of 5.0) was used as a sintering atmosphere. The flow-rate of the processing atmosphere was 4 l/min. Atmosphere drying was performed utilizing zeolite molecular sieve dryers. The inlet dew point (monitored by the SHAW Super-Dew Hygrolog) was about -59°C.

Specimens selected for metallographic analysis were polished with 0.1μm diamond paste and etched in 2% nital solution. The microstructure of specimens was investigated using the optical microscope (OLYMPUS GX71, Japan) and the scanning electron microscope coupled with the energy dispersive spectrometer (JEOL JSM-7000F, Japan with EDX INCA).

Corrosion of samples in the Hank's solution, composed of (in g/l) 8.00 NaCl, 1.00 Glucose, 0.60 KH_2PO_4, 0.40 KCl, 0.35 $NaHCO_3$, 0.14 $CaCl_2$, 0.10 $MgCl_2$ $6H_2O$, 0.06 $MgSO_4$ $7H_2O$, and 0.06 NaH_2PO_4 $2H_2O$ with a pH value of 7.4, was investigated. Measurements were carried out by the use of the Autolab Potentiostat PGSTAT 302N in a conventional three-electrode arrangement with the Ag/AgCl reference electrode, platinum counter electrode and iron or iron-phosphorus sample as the working electrode. In all experiments, the temperature of electrolyte was maintained at $37^oC\pm1^oC$. Before the potentiodynamic polarization tests started, the samples were kept immersed in the electrolyte for 1 h and the temporal evolution of the open-circuit potential (OCP) was recorded. After an hour the potentiodynamic measurements started. Polarization curves were obtained by varying the applied potential from -800 mV up to -200 mV at the scan rate of 0.1 mV/s. The Higuchi's algorithm was used to probe whether the recorded OCP time series were fractals and to estimate their fractal dimension. Corrosion current, corrosion potential and corrosion rate were determined from polarization curves by the use of the Tafel extrapolation technique.

3. RESULTS AND DISCUSSION

3.1. Microstructure of sintered compacts

The microphotographs in Fig.1 present the microstructure of Fe and Fe-0.5P samples and those in Fig.2 show the microstructure of Fe-1.0P sample after sintering lasted for 60 min at 1050^oC. It is

evident that the liquid phase was created during sintering due to interactions in the Fe_2O_3-P_2O_5 system [8].
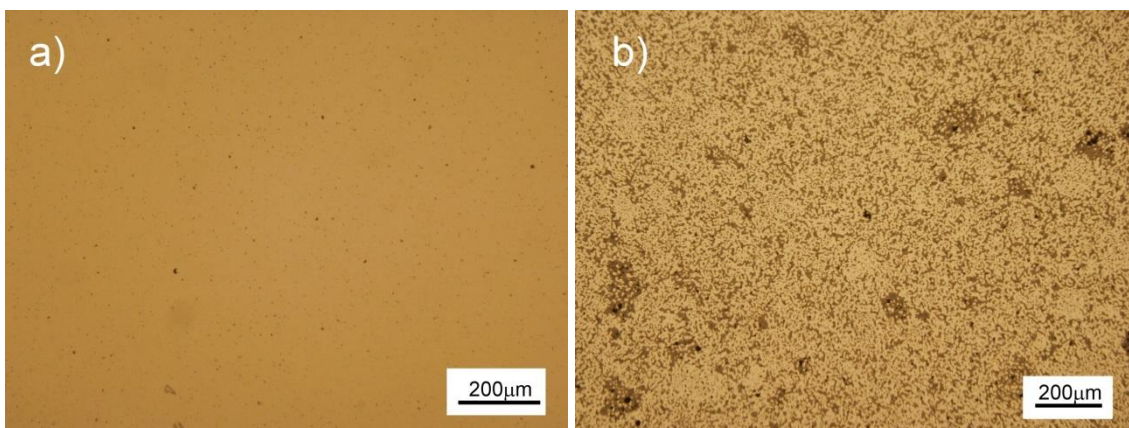

Figure 1. SEM micrographs of polished sections of Fe (a) and Fe-0.5P (b) sintered compacts showing their different microstructures.
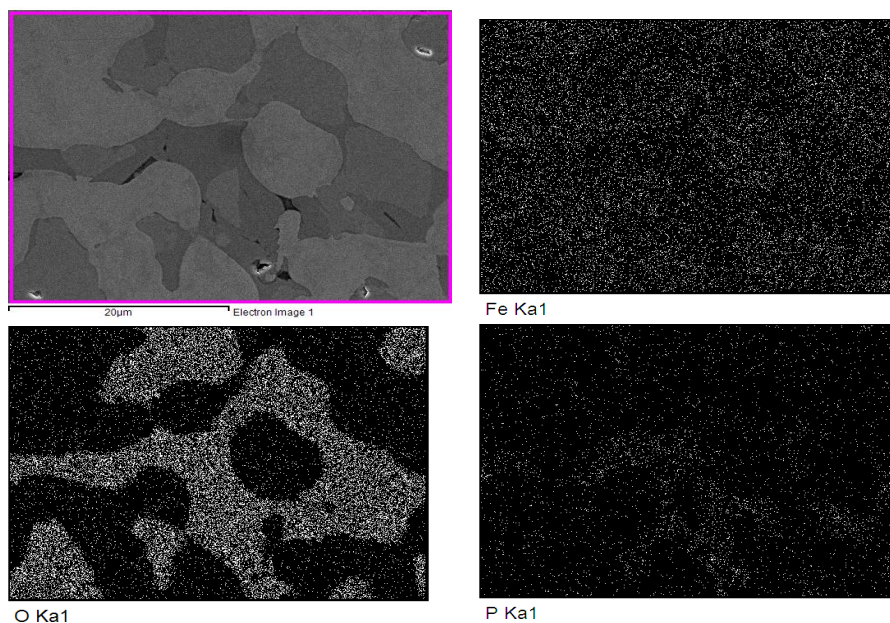

Figure 2. A SEM micrograph of a polished section of Fe-1.0P sintered compact showing its microstructure, and the EDX mapping of the distribution of iron, oxygen and phosphorus within this microstructure.

The liquid-phase assisted sintering has led to the structure consisting of more or less interconnected network of spheroidized particles, which remained solid during sintering, surrounded by (or „immersed" in) the solidified liquid phase (Fig.2). Spheroidized particles were of two kinds: either from α-Fe phase (light grey) or from iron oxides (darker grey). The solidified liquid phase (dark

grey up to black colour) consisted of ferric phosphate compounds resulting from the interactions in the Fe_2O_3-P_2O_5 system ($FePO_4$, Fe_3PO_7, $Fe_4(P_2O_7)_3$, $Fe(PO_3)_3$,...).

3.2 Electrochemical corrosion behaviour

Fig.3 presents the ways in which the open-circuit potentials (OCP) of the tested electrodes varied with time after immersion in the Hank's solution. At the beginning, the electrode from Fe possessed the highest open-circuit potential, and the potential of the electrode from Fe-1.0P was the lowest one. A quite rapid continuous reduction of potential of the Fe electrode freely corroding in the in Hank's solution was observed during the test. And after about 2400 seconds, the OCP of the Fe electrode became lower than that of the Fe-0.5P electrode but remained still higher than OCP of the Fe-1.0P electrode. An air-formed primary oxide film on the sample surface, which to some extent protected the iron material, was dissolved during the test which made the iron more prone to corrosion.
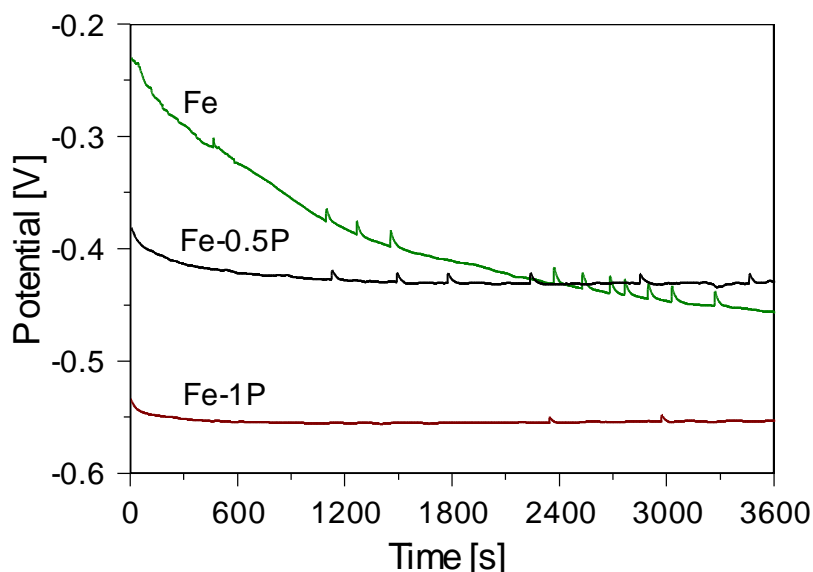

Figure 3. The temporal evolution of the open-circuit potential of Fe, Fe-0.5P, Fe-1.0P electrodes immersed in the Hank's solution.

The open-circuit potentials exhibited cathodic transients, the sharp increases in potential of about centivolt magnitude followed by an exponential-type recovery over a short time period. Analogous positive-going potential transients observed for carbon steels were associated with the stress corrosion cracking process [9,10].

After a crack propagation has been initiated, the freshly exposed iron surface is highly catalytic and is able to catalyze the reduction of adsorbed water to hydroxyl ions and hydrogen atoms. This fast cathodic reaction consumes electrons that are supplied by a discharge of the electrode. This results in

a spontaneous polarization of the electrode to a more noble value measured as a positive-going potential transient. The metal-electrolyte interface is then recharged by a subsequent metal dissolution.

As sintered samples usually contain internal residual stresses, the stress corrosion cracking can be responsible for positive-going potential transients in our case too.

When we look at the OCP versus time graphs at no better than centivolt resolution, the open-circuit potentials recorded for Fe-P systems seem to be more smoother functions of time than the one recorded for Fe, as it is shown in Fig.3. But the situation changes under higher and higher resolution, when the OCP time series tend to appear rather rugged and reveal an irregular structure (Fig.4). Such an irregular OCP time series, regarded as a subset of the (time, potential)-coordinate plane, may be a fractal. To verify whether the OCP time series are really fractals and to estimate their fractal dimensions, the Higuchi's method was used.
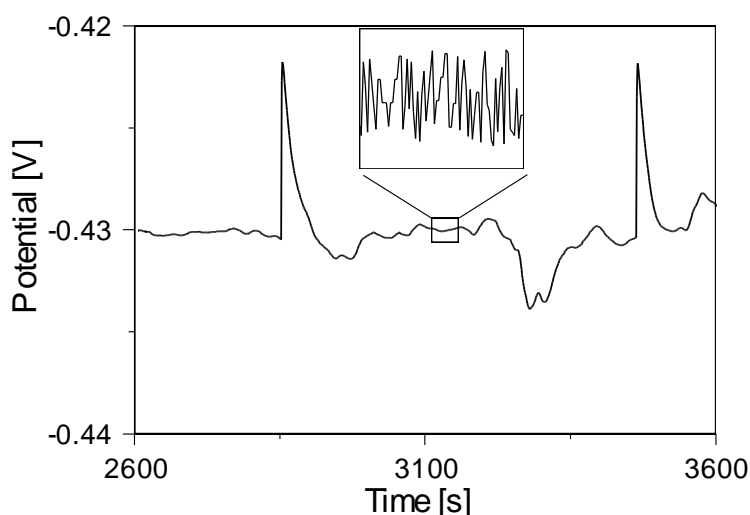

Figure 4. Zooming into the temporal evolution of the open-circuit potential of Fe-0.5P electrode to reveal a finer structure.

The Higuchi's estimator [11] was chosen as it is one of the most robust method to compute the fractal dimension of discrete time series and provides the most accurate estimates of this dimension [12]. This algorithm is briefly sketched below.

Consider $X(1)$, $X(2)$,…,$X(N)$ the time sequence to be analysed. From a given time series, k new time series X_m^k are constructed, defined as follows:

$$X_m^k = \left\{ X(m), X(m+k), X(m+2k),..., X(m + n_{li}(N,m,k)k) \right\} \qquad \text{for } m=1,2,…,k.$$

Here $n_{li}(N,m,k)$ stands for the lower integer part of $(N-m)/k$. m indicates the initial time value, and k represents the discrete time interval (delay) between points. For a time interval equal to k, one

gets *k* sets of new time series. For each of the curves or time series X_m^k, the length of the curve is defined as follows:

$$L_m(k) = \frac{N-1}{n_{li}(N,m,k)k^2} \sum_{i=1}^{n_{li}(N,m,k)} |X(m+ik) - X(m+(i-1)k)|.$$

The term $(N-1)/n_{li}(N,m,k)k^2$ represents the normalization factor for the curve length of subset time series. The length $<L(k)>$ of the curve for the time delay *k* is defined as the average value of *k* lengths $L_m(k)$. If $<L(k)> \propto k^{-D}$, then the curve analysed is fractal with the dimension *D*.

Figure 5 shows the results of "fractal geometry" analysis of the time records of the OCPs of investigated electrodes. The analysis confirmed that for each of the measured samples the temporal evolution of open-circuit potential yielded a time series which was a fractal in the (time, potential)-coordinate plane with the fractal dimension *D*>1. For Fe electrode *D*=1.14, for Fe-0.5P electrode *D*=1.51, and for Fe-1.0P electrode *D*=1.52.
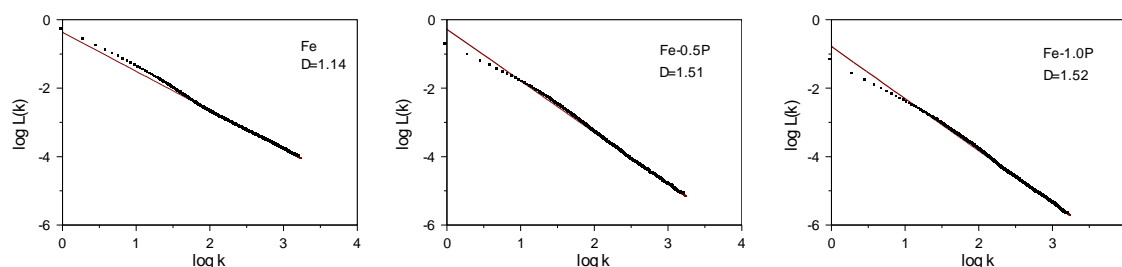

Figure 5. The results of Higuchi's algorithm applied to OCP time series. In that context, *k* represents the discrete time interval between points constituting a particular subset of time sequence being analysed, and *L(k)* is the average value of the length of the OCP time series defined on the time subsequence with time delay *k*. *D* represents the corresponding fractal dimension of the OCP time series.

In the simplest case of corrosion, the numerous very tiny corrosion cells are distributed in a random manner over the surface of the metallic electrode, with anodic and cathodic sites which „travel" all the time from one place to another one. The overall effect is the uniform corrosion [13]. The corrosion potential results from the superposition of contributions from many more or less independent surface corrosion events. The particular temporal evolution of the corrosion potential of the electrode undergoing uniform corrosion may be therefore treated as a realization of the stochastic Gaussian process. The Gaussian noise yields a time series with a fractal dimension of 1.5 [14,15].

For the Fe-0.5P and Fe-1.0P electrodes, the fractal dimensions of OCP time series were found to be of 1.51 and 1.52, respectively. This indicates that those samples could undergo nearly uniform (or general) corrosion. That may be the case, because in the Fe-P systems, with various phases randomly distributed in the sample and concentrations of alloying elements randomly varying over the

surface, numerous small temporal galvanic couples can appear, disappear, and wander all over the surface as the metal dissolution is ongoing.

As regards the Fe electrode, the fractal dimension of its OCP time series was of 1.14, which is clearly less than 1.5. So the corrosion potential of Fe electrode evolved as if it was a fractional Gaussian noise with the Hurst exponent of 0.86. Thus, the fluctuations of OCP value of our Fe sample should be positively correlated with long memory effect. That is, the data values going in some direction tend to be followed by data values going in the same direction with respect to the mean value [14,15]. This is consistent with what is expected from the corrosion dominated by the stress corrosion cracking events, as one increment in the crack length raises the probability of another one in later time, both yielding the positive-going potential transients.

Degradation rates of tested materials immersed in the Hank's solution were estimated from potentiodynamic polarization curves. The reproducibility of Tafel plots was good. The corrosion potential (E_{corr}) and corrosion current density (i_{corr}) were calculated from the intersection of the anodic and cathodic Tafel lines extrapolations, and the corrosion rate (R_M) was estimated according to ASTM G 102-89 [16].

It was assumed that the samples corroded uniformly and the process of oxidation did not occur selectively for any component of the alloy. When the non-uniform corrosion processes were occurring, the above result underestimates the true value of the corrosion rate.

All values of E_{corr} , $i_{corr,}$ R_M, the anodic (b_a) and cathodic (b_c) Tafel slopes are summarized in Tab.1. The addition of 0.5wt.% of P to the carbonyl iron resulted in a higher (more noble) steady-state corrosion potential. This positive shift (with respect to a pure iron) indicates the decreased corrosion susceptibility of iron samples containing 0.5wt.% of P (Fig.6.). The addition of 1.0wt.% of P caused the negative potential shift in comparison with the iron sample. This negative shift indicates the increased tendency of these samples to corrode (Fig.6.).
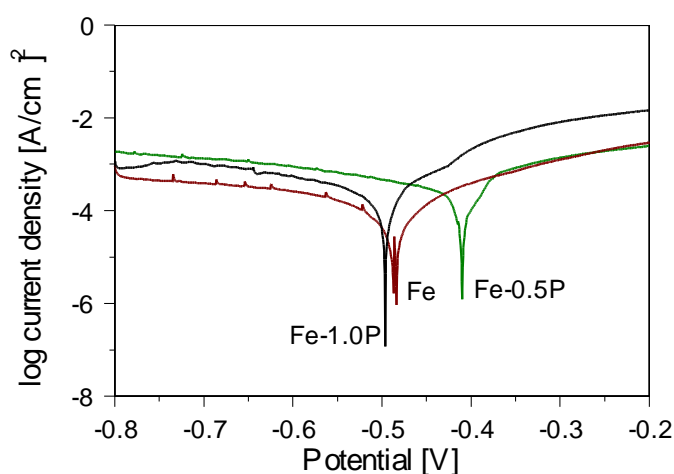

Figure 6. Polarization curves for iron and iron-phosphorus samples immersed in the Hank's solution.

The corrosion potential can be shifted to a less noble value if a significant fraction of iron atoms find themselves at higher energy sites because of an altered surface topography, a more

heterogeneous microstructure of surface, longer and more rugged boundaries between different phases, etc. An attempt to explain the observed potential shifts is outside the scope of the article.

Table 1. The values of E_{corr}, i_{corr}, b_a, b_c and corrosion rates obtained for Fe, Fe-0.5P and Fe-1.0P sintered specimens immersed in the Hank's solution

Sample	E_{corr} [mV]	b_a [mV/dec]	b_c [mV/dec]	i_{corr} [A/m^2]	Corrosion rate [mm/year]
Fe	−484	45	42	0.15	0.20
Fe-0.5wt.%P	−403	34	23	0.44	0.69
Fe-1.0 wt.%P	−497	36	43	0.45	0.71

The corrosion current density (i_{corr}) measured for Fe sample was approximately three times lower than i_{corr} measured for Fe-0.5P and Fe-1.0P samples. The difference in corrosion current densities between Fe-0.5P and Fe-1.0P samples was negligible and the difference in corrosion rates calculated from these corrosion current densities was not significant. Thus the corrosion resistance of Fe samples was found higher than that of any Fe-P sample, though, according to corrosion potentials, the lowest tendency to corrode was found for the Fe-0.5P sample.

The measured anodic Tafel slopes ranged from 34 mV/dec to 45 mV/dec, and cathodic Tafel slopes ranged from 23 mV/dec to 43 mV/dec.

As the investigated quite heterogeneous electrodes corrode, metal dissolution, oxygen reduction, hydrogen evolution, … , take place simultaneously. These processes usually involve various multi-step reactions, with steps of various rates and transferring various numbers of electrons, which can result in a variety of measured Tafel slopes. For example, the Heusler mechanism of iron dissolution [17], which assumes that OH^- ions participate in reaction during which the $FeOH_{ads}$ and $FeOH^+$ are subsequently formed, involves three-step dissolution with the second step being rate-determining, in which two electrons are simultaneously transferred. For 37°C this mechanism yields an anodic Tafel slope about 44 mV per decade [17]. But the identification and analysis of electrode reaction mechanisms are outside the scope of this article and are the subjects of future studies.

4. CONCLUSIONS

The carbonyl iron and carbonyl iron-phosphorus samples were prepared by a powder metallurgy to investigate the effect of addition of 0.5 wt.% and 1.0wt.% of P to the iron powder on the microstructure and in vitro electrochemical degradation of prepared sintered samples.

The obtained microstructure can be described as a spatial network of spheroidized particles from iron or iron oxides surrounded by a solidified liquid phase consisting of a variety of ferric phosphates.

When immersed in the Hank's solution, the corrosion potential of a freely corroding iron sample persistently decreased with time, with sudden positive potential transients occurring from time

to time, while the corrosion potentials of Fe-P samples had decreased during the first ten minutes and then became nearly constant functions of time, with potential transients occurring less frequently. This indicated the localised corrosion of iron sample (probably through stress corrosion cracking processes) and more uniform corrosion of Fe-P samples.

The application of Higuchi's estimator to the recorded OCP data confirmed that the temporal evolution of open-circuit potentials yielded the time series which were fractal objects. Time series generated by fluctuating corrosion potentials of Fe-P electrodes possessed the fractal dimensions very close to 1.5. Fractal dimensions near to 1.5 accord with an idea that the corrosion potential represents a superposition of contributions from a lot of miniature corrosion events which are statistically independent of each other. Such a situation is usually associated with a uniform corrosion.

Fluctuations of corrosion potential of the Fe-electrode yielded a time series with the fractal dimension of 1.14. This can indicate that the corrosion potential is a superposition of contributions from predominantly positively correlated corrosion events. Such a situation can be associated with the stress-corrosion-cracking form of localised corrosion, for example.

It was found that the addition of 0.5 wt.% of P resulted in a positive shift of the steady-state corrosion potential and the addition of 1.0wt.% of P resulted in a slight negative shift of the corrosion potential of the electrode immersed in the Hank's solution with respect to the corrosion potential of undoped iron. The obtained electrochemical data showed that the corrosion rate increased from Fe, through Fe-0.5P to Fe-1.0P material. A porous structure of sintered iron sample allowed degradation rate to increase with respect to a „bulk" iron.

It is worth noting that though the Fe-0.5P sample showed the lowest tendency to corrode (the most positive corrosion potential), its corrosion rate is similar as that of the Fe-1.0P sample which is clearly most prone to corrosion (the most negative corrosion potential).

A detailed explanation of observed phenomena lies beyond the scope of the article presented. A deeper understanding of the degradation of PM iron-phosphorus biomaterials in simulated body fluids, as well as the verification of the usefulness of the fractal geometry for the analysis of corrosion phenomena, represent the goals for the further investigation.

References

1. Y. Yun, Z. Dong, N. Lee, Y. Liu, D. Xue, X. Guo, J. Kuhlmann, A. Doepke, H.B. Halsall, W. Heineman, S. Sundaramurthy, M.J. Schulz, Z. Yin, V. Shanov, D. Hurd, P. Nagy, W. Li, 12 *Materials Today* (2009) 22
2. H. Hermawan, D. Dubé, D. Mantovani, *Acta Mater.* 6 (2009) 1693
3. H. Hermawan, D. Dubé, D. Mantovani, *J. Biomed. Mate. Res. Part A* 93 (2010), 1
4. H. Hermawan, A. Purnama, D. Dube, J. Couet, D. Mantovani, *Acta Biomater.* 6 (2010) 1852
5. P. Quadbeck, R. Hauser, K. Kümmel, G. Standke, G. Stephani, B. Nies, S. Rössler, B. Wegener, *Proc. Powder Metallurgy World Congress & Exhibition, PM 2010*, Vol.2 (2010) 239

6. B.Wegener, B. Sievers, S. Utzschneider, P. Müller, V. Jansson, S. Rößler, B. Nies, G. Stephani, B. Kieback, P.Quadbeck, *Mater. Sci. Eng. B* 176 (2011) 1789
7. H. Bruncková, M. Kabátová, E. Dudrová, *Surf. Interface Anal.* 42 (2010) 13
8. M. Kabátová, E. Dudrová, H. Bruncková, *Surf. Interface Anal.* 45 (2013) 1166
9. H.J. DeBruyn, K. Lawson, E.E. Heaver, *Electrochemical Noise Measurement for Corrosion Applications* Issue 1277, ASTM International, West Conshohocken, PA. (1996) 214
10. J. L. Dawson, *Electrochemical Noise Measurement for Corrosion Applications* Issue 1277, ASTM International, West Conshohocken, PA. (1996) 3
11. T. Higuchi, *Physica D* 31 (1988) 277
12. P. Simard, E. La Tavernier, *Mechan. Syst. Signal Processing* 14 (2000) 459
13. E. McCafferty, *Introduction to Corrosion Science*, Springer Science + Business Media, New York, (2010)
14. P.S. Addison, *Fractals and Chaos: An Illustrated Course*, IOP Publishing, Bristol, (1997)
15. D.L. Turcotte, *Fractals and Chaos in Geology and Geophysics* second edition, Cambridge University Press, Cambridge, (1997)
16. ASTM G102-89, *AST International*, West Conshohocken, PA (2010), www.astm.org
17. D. Landolf, *Corrosion and Surface Chemistry of Metals*, EPFL Press, Lausanne (2007)